Applied Surface Science Advances 2 (2020) 100034

Contents lists available at ScienceDirect

Applied Surface Science Advances

journal homepage: www.elsevier.com/locate/apsadv

Influence of base pressure prior to deposition on the adhesion behaviour of carbon thin films on steel

Carla D. Boeira[a], Leonardo M. Leidens[a], Alexandre F. Michels[a], Ricardo Serra[b], Manuel Evaristo[b], Filipe Fernandes[b], Albano Cavaleiro[b,c], Carlos A. Figueroa[a,d,*]

[a] PPGMAT, Universidade de Caxias do Sul, 95070-560 Caxias do Sul, RS, Brazil
[b] Universidade de Coimbra, CEMMPRE, 3030-788 Coimbra, Portugal
[c] LED&Mat-IPN, Instituto Pedro Nunes, 3030-199 Coimbra, Portugal
[d] Plasmar Tecnologia Ltda., 95030-775 Caxias do Sul, RS, Brazil

ARTICLE INFO

Keywords:
Base pressure
Adhesion
DLC
Oxygen pressure
Delamination
Scratch test
EDS mapping

ABSTRACT

The poor adhesion of carbon thin films was the main restriction for its massive application in recent years. Physicochemical interaction improvement at the adhesion interface between substrate and thin film is one of the most important fields of research to overcome such problem. From a chemical point of view, oxygen seems to be a major issue in the adhesion control. In this work, the influence of base pressure prior to deposition process on the carbon thin film tribological behaviour was studied. Rockwell C and scratch tests were performed to qualify the thin film failures and adhesion. Chemical mapping was performed by energy-dispersive spectroscopy to characterise the chemical elements after thin film failure. The carbon thin films show better adhesion at lower base deposition pressures. The tribological behaviour is associated with the oxygen content in the chamber atmosphere as well as to the higher thin film adhesion achieved at lower base pressures.

1. Introduction

Poor adhesion of carbon thin films on ferrous alloys restricts many industrial applications regarding their mechanical and tribological properties [1]. Carbon thin films are usually applied in engine and mechanical components to effectively reduce the friction and wear of the sliding parts [2,3]. However, the high residual stress of such coatings is the main technical restriction for their massive applications [4,5]. Chemical vapour deposition (CVD), physical vapour deposition (PVD) and plasma-enhanced chemical vapour deposition (PECVD) techniques provide relatively large ion fluxes on substrate for the growth of carbon thin films and are consolidated at the laboratorial scale [6,7]. For industrial processes, magnetron sputtering (MS) techniques are employed for their conceptual simplicity and their ability to deposit uniform and low- defect films. However, magnetron sputtering plasmas in DC, pulsed and RF configurations are characterised by relatively low electron densities that may induce poor mechanical and adhesive properties [8,9]. High-power impulse magnetron sputtering (HiPIMS) technique shows a high ionisation rate of plasma species at high power that allow ion implantation during deposition, which improves the density and adhesion of thin films. In addition, carbon is difficult to be ionised. Studies have reported the possibility of improving the deposition rate exploring both the experimental setup and the deposition conditions [10,11]. Non-metallic and metallic interlayers are used to improve the adhesion of carbon thin films enhancing the poor chemical bonding and mismatching at the interface [12]. These interlayers have scientific and industrial importance and can be easily obtained using the above-mentioned techniques. Interlayers aim to reduce the physical and chemical incompatibilities between the carbon thin film and the ferrous substrate, incompatibility that is responsible for the poor adhesion to the system thin film/substrate. Elements such as Ti, Cr, F, B, S, Si and N are generally used at the interlayer and should be, consequently, compatible [13–15]. Otherwise, these elements become the main initiator of failure and of delamination [16,17]. Previous studies have reported that Si-containing interlayers improve the adhesion in thin film//steel systems [18–20]. In this case, it should be remarked that a new interface is created in the final sandwich architecture of thin film//interlayer//steel. The better adhesion does not depend only on the silicon concentration but also on the chemical structure of the functional groups created during thin film processing which are associated with the deposition parameters [21–23]. The Si-C bonds promoted by the carbon thin film//Si-containing interlayer system are effective in reducing internal stress and improving adhesion [24,25].

---

* Corresponding author at: PPGMAT, Universidade de Caxias do Sul, 95070-560 Caxias do Sul, RS, Brazil.
E-mail address: cafiguer@ucs.br (C.A. Figueroa).

https://doi.org/10.1016/j.apsadv.2020.100034
Received 31 August 2020; Received in revised form 20 October 2020; Accepted 16 November 2020

Table 1
Code of samples, pumping times and pressures for deposition processes.

Sample	Pumping time (min)	Base pressure (Pa)	Estimated oxygen partial pressure (Pa)
10^{-1}	10	1.6×10^{-1}	3.10×10^{-2}
10^{-2}	40	1.0×10^{-2}	2.08×10^{-3}
10^{-3}	100	1.7×10^{-3}	3.40×10^{-4}
10^{-4}	200	2.2×10^{-4}	4.40×10^{-5}

A Si-containing adhesion interlayer must present good thermal and structural stability, which is able to be reached after the formation of strong Si-C bonds between Si, from the adhesion interlayer, and C, from the carbon thin film [26]. On the one hand, previous works have reported that the oxygen presence, as a dopant element in carbon thin films, has a major role in their tribological performance [26–28]. Moreover, other works have concluded that the oxygen presence at interfaces jeopardises the adhesion of carbon thin films on ferrous alloys becoming a key factor [29,30]. The oxygen presence at the interfaces of the carbon thin film//interlayer//ferrous alloy system comes from either the residual gases absorbed on the walls or the residual air into the chamber during plasma deposition [31]. Different methods to remove or minimise the oxygen content have been proposed, such as, the use of a relatively high deposition temperature or hydrogen etching [32,33]. However, there is a lack of systematic studies to evaluate the influence of the chamber base pressure on the adhesion of carbon thin films on ferrous alloys without any other treatment. Consequently, this work aims to investigate the influence of the deposition base pressure on the adhesion behaviour of carbon thin films deposited on ferrous substrate.

2. Material and methods

Samples of AISI M2 steel~~,~~ with diameter of 21.5 mm and thickness of 4 mm were polished with SiC abrasive paper followed by diamond suspension of 3 μm and, after, were ultrasonically cleaned with acetone and ethanol baths for 15 min. The samples were glued with silver glue (99.9% purity) and placed on a rotating holder with rotation of 18 rpm at the central axis of the chamber and situated to 80 mm distance from the targets. The deposition chamber is a vacuum system constituted by a rotary (Edwards NxOs 20i) and a turbomolecular pumps (Pfeiffer TMH 521 P) sealed with Viton® rubber. This equipment is located in the clean room with controlled temperature and humidity. The first stage of the deposition process was the chamber evacuation where different pump times allow reaching each base/background pressure, i.e., the vacuum level achieved before starting the silicon interlayer and carbon film depositions. The longer the pumping time, the lower the base pressure. This base pressure was the main parameter to be studied in this work and, therefore, Table 1 describes the different times to evacuation and deposition base pressures where the estimated oxygen partial pressures, which consider only air (rough approximation) in the base pressure, are also shown. Different pumping times render different base pressures prior to deposition of the silicon interlayer and subsequent carbon thin film. The coatings were deposited at room temperature with using direct current magnetron sputtering under Ar (99.999%) atmosphere (constant pressure of 0.5 Pa with a flow rate of 21 sccm). The etching stage was used to remove all surface contaminants and activate the surface. After etching, a Si interlayer was deposited by sputtering using a pure Si target (150 × 150 mm). The carbon thin film was then deposited by sputtering a graphite target (150 × 150 mm) [34,35] until a final thickness of 0.3 μm is achieved. Detailed process parameters for deposition process are described in Table 2.

The adhesion behaviour of the carbon thin films was evaluated using adhesion tests: Rockwell C indentation test and the instrumented linear scratch-test. The chemical composition was analysed by Energy Dispersive Spectroscopy (EDS) technique. The Rockwell indentation test, also known as "Mercedes test", was performed using a Rockwell C indenter under a normal load of 1471.5 N (recommended for AISI M2 substrate) using Karl Frank GMBH Weinheim-Birkenau Type 38 532 equipment. The indentations were categorised into six failure classes in order to evaluate the adhesion strength and the type of fracture of carbon thin films according to VDI 3198 indentation test [36,37]. The instrumented linear scratch-test (Swiss CSEM Scratch Test) was conducted according to European Standard EN 1071-3 [38] by linearly applying loads from 0 to 50 N on a trail length of 50 mm, using a Rockwell C with a tip (Mössner Ideen Aus Diamant) radius of 200 μm. The worn trail as well as the Rockwell indents were evaluated by optical microscopy (OM) using a Leica DM4 B vertical microscope to assess the failure and delamination mechanisms. Scanning electron microscopy (SEM-Shimadzu SSX-550) was also used to evaluate the delamination mechanisms. The chemical mapping in qualitative mode was determined in the same SEM focusing in the same area that those for microstructural analysis by EDS (Oxford X-act).

Table 2
Processing parameters for sample deposition.

	Argon etching	Si interlayer	Carbon-based thin film
Time (min)	30	10	20
Target	–	Si	graphite
Voltage (V)	–	450	650
Bias (V)	250	60	60
Power (W)	130	550	750

3. Results and discussion

Fig. 1(a)–(d) shows OM images after Rockwell C indentation of thin films deposited at variable base pressure. Different adhesion/cohesion behaviours are observed as a function of the deposition base pressure. Carbon thin films deposited at relative high base pressures of 1.6×10^{-1} and 1.0×10^{-2} Pa were ultimately removed as shown in Fig. 1(a) and (b), respectively. At intermediate deposition base pressure of 1.7×10^{-3} Pa (Fig. 1(c)) the adhesion is enhanced and only microcracks and isolated small delamination areas were detected. The lowest deposition base pressure (2.2×10^{-4} Pa) guaranteed good adhesion of the carbon thin films where only minor microcracks are seen (Fig. 1(d)). According to the standard VDI 3198 [36], the adhesion can be classified through cracking and coating delamination around the indent [39]. Fig. 1(e)–(h) shows the OM images at higher magnification around the indentation for each sample. Consequently, the adhesion/cohesion behaviour of carbon thin films as a function of deposition base pressure is able to be matched to the standard VDI 3198, accordingly. This classification is ranked from HF1 to HF6 where the area around the indentation is classified as HF1 and HF2, for a suitable adhesion when just a few cracks are observed, HF3 to HF5 is associated with delamination and massive cracking points and, HF6, corresponds to a complete delamination [40]. Fig. 1(i)–(l) shows EDS analyses of carbon (C) and silicon (Si) in the carbon thin film and interlayer systems deposited on AISI M2 steel after Rockwell C indentation for different base pressures. These figures identify, qualitatively, the presence of carbon (in red colour) and silicon (in blue colour) in the cracks and delamination points created due to indentations. According to images in Fig. 1, and the standard classification for Rockwell C analysis, these samples were classified as follows: HF6 for the samples deposited at base pressures of 1.6×10^{-1} and 1.0×10^{-2} Pa, since these images show complete delamination of

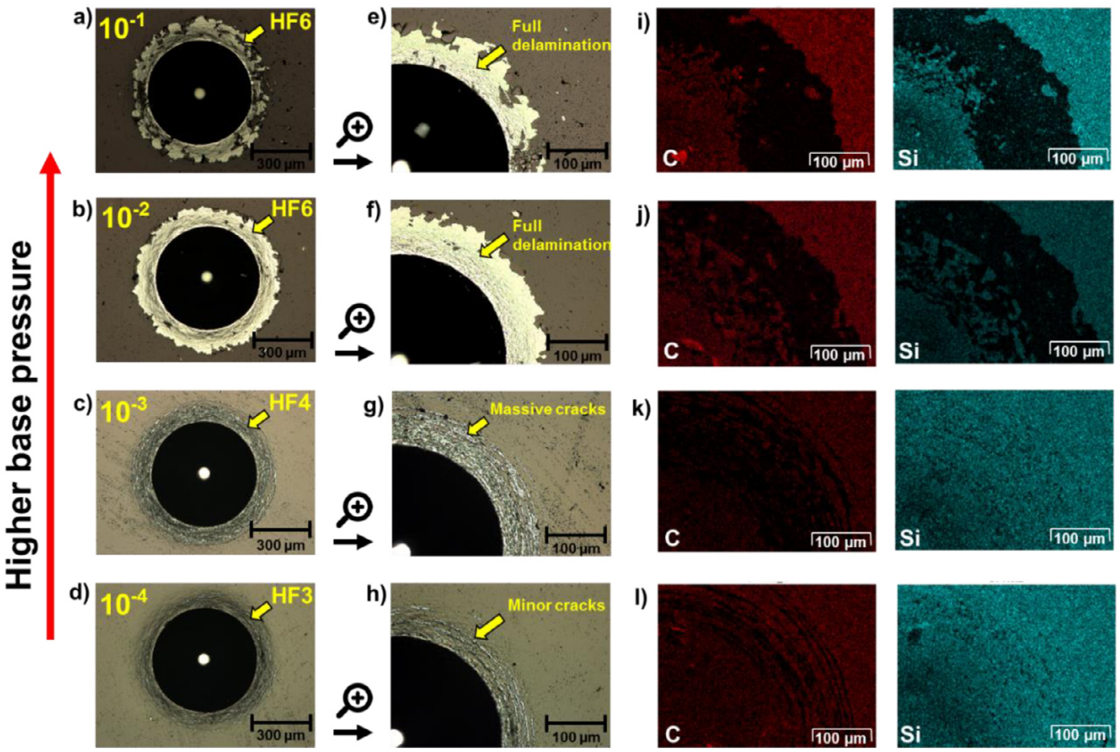

Fig. 1. (a)–(d) Optical microscopy images of top view Rockwell C indentation areas for samples deposited at high base pressure (at the top) to low base pressure (at the bottom); where (e), to (h) detailed the optical microscopy images of cracking region and delamination mechanisms (i) to l) EDS analyses of C and Si chemical elements in the sandwich structure of carbon thin film//interlayer//steel after Rockwell C indentations at variable deposition base pressures. (For interpretation of the references to colour in this figure, the reader is referred to the web version of this article.)

both the carbon thin film and silicon interlayer, exposing the metallic material as seen in Fig. 1(i) and (j) where no carbon and silicon signals were recorded in the delaminated zone; HF4 for the sample deposited at base pressure of 1.7×10^{-3} Pa, showing massive cracking points and local delamination and, finally, the sample deposited at base pressure of 2.2×10^{-4} Pa was classified as HF3 due to the much lower number of cracks. For these last two base pressures, only the carbon thin film was delaminated remaining the silicon interlayer as shown in Fig. 1(k) and (l).

Fig. 2(a) schematises the linear scratch-test conducted by linearly applying loads from 0 to 50 N on a trail length of 50 mm. Fig. 2(b) shows the OM images of worn trails after testing of carbon thin films as a function of the deposition base pressure. Higher magnification and chemical mapping of worn trails are shown in Fig. 2(c) where the different failure types may depend on the base pressure. Typical cohesion (buckling) and adhesion (lateral chipping and spalling) failures of the carbon thin films [40] are observed in the micrographs. The arrows in Fig. 2(b) indicate the critical load determined at the beginning of coating detachment and complete failure. Delamination failures (spalling) are observed for samples deposited at the highest base pressures where the failure occurs aggressively at low normal forces, exposing a large area of delamination. The higher magnification obtained in Fig. 2(c) by SEM allows to analyse the delamination mechanism at the beginning with more details. For samples deposited at high deposition base pressures (codes: 10^{-1} and 10^{-2}), the failure starts by cohesive failure, with cracking induced by buckling, occurring delamination of both carbon thin film and silicon interlayer. For the sample deposited at lower deposition base pressures (codes: 10^{-3} and 10^{-4}), the delamination occurs at much higher forces, in a milder manner keeping the silicon interlayer (see the presence of silicon in the delaminated areas for conditions 10^{-3} and 10^{-4} in Fig. 2(c). As mentioned above, a lower deposition base pressure enhanced the adhesion behaviour, requiring higher critical loads for the delamination to occur. One must notice that the brighter points for silicon on EDS chemical maps in Fig. 2(c) should be associated with rich-W metallic carbides precipitates in the substrate (AISI M2). Indeed, the Si K-$L_{2,3}$ and W M_5-$M_{6,7}$ peaks show photon energies at 1.740 and 1774 eV [41], respectively. Thus, the brighter signal for silicon in Fig. 2(c) is due to an extra signal that comes from tungsten.

The dependence of the critical load for delamination of carbon thin films on the deposition base pressure is presented in Fig. 3. As the deposition base pressure decreases, the critical load increased from 9 N to about 27 N. Therefore, the base pressure reduction significantly improved the cohesion/adhesion behaviour. We did not consider the humidity for this discussion because and as mentioned in the experimental section, all samples were processed in an equipment sealed by Viton® rubber, which may leak water vapour from room atmosphere to chamber atmosphere. Moreover, the equipment for thin film deposition is located in a clean room with controlled environmental conditions of temperature and humidity, thus, the background condition can be considered constant in terms of the atmospheric composition and relative humidity when the deposition chamber is closed and during pumping [42]. The residual chamber atmosphere is, majorly, constituted by atmospheric air (~ 78 of N_2 and ~ 21% of O_2) and water vapour. In terms of reactivity, oxygen that comes from oxygen and water molecules is more dangerous than nitrogen in plasma-based processing and, in addition, oxygen is known as a potential barrier to appropriate adhesion of carbon coatings in a chemical point of view [31,43]. One must notice that our results can only be correlated with the deposition base pressure and our discussion about the harmful effect of residual oxygen, which is one of the strongest hypotheses, must be proven by quantitative chemical analysis that is beyond the scope of the current work.

Fig. 4 proposes a delamination mechanism for the sandwich structure of the thin film//interlayer//steel occurring during scratching in two different failure modes that depend on a) high (codes: 10^{-1} and 10^{-2})

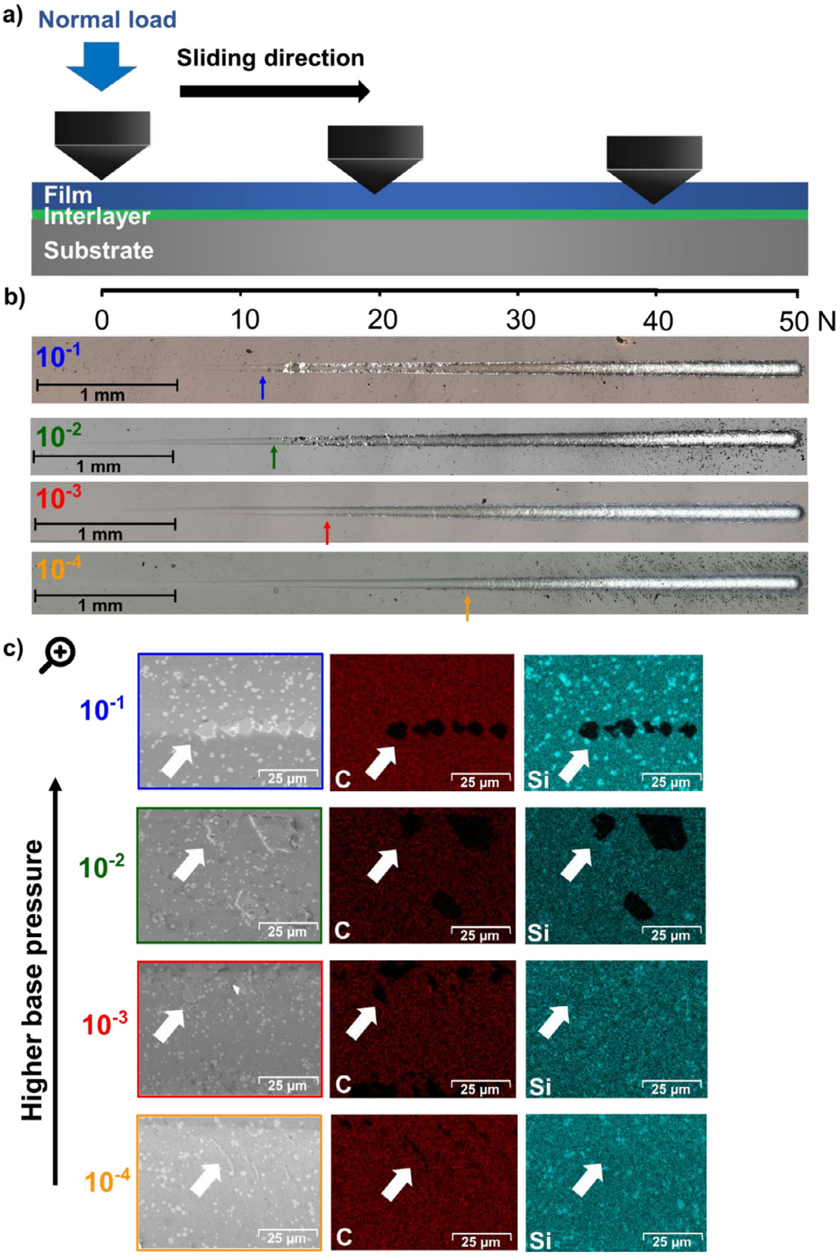

Fig. 2. (a) Schematic of the linear scratch-test, (b) OM images of worn trails after instrumented linear scratch-testing for samples, (c) SEM and EDS analyses of characteristic areas to evaluate the first stages of delamination during scratching.

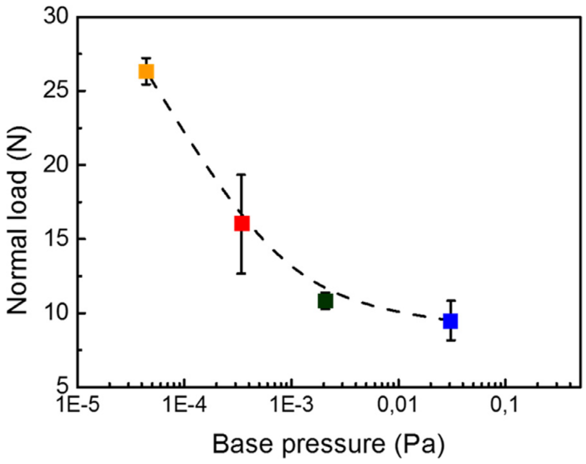

Fig. 3. Critical load for thin film delamination at variable base pressure during deposition. The dashed line is a guide line for the eyes.

or low b) (codes: 10^{-3} and 10^{-4}) deposition base pressures. Fig. 4(a) shows that high deposition base pressures induce delamination at the innermost interface, i.e., at the silicon interlayer and steel interface exposing the substrate. Fig. 4(b) shows that low deposition base pressures induce delamination at the outermost interface, i. e., at the carbon thin film and silicon interlayer interface exposing the silicon interlayer. We suggest that this behaviour may be associated with the oxygen partial pressure during deposition since both air and water vapour (possible origin of oxygen in the interface) are mostly evacuated during pumping to reach the deposition base pressure [42]. Moreover, the equipment for thin film deposition is located in a clean room with controlled environmental conditions of temperature and humidity, thus, the background condition can be considered constant in terms of the atmospheric composition when the deposition chamber is closed. After that, different base/background deposition pressures are achieved, which define our systematic study. The better cohesion/adhesion behaviour of the carbon thin films on AISI M2 steel is associated with the low deposition base pressure, which may be associated with the presence of oxygen during the deposition process. Previous works have shown that the chemical

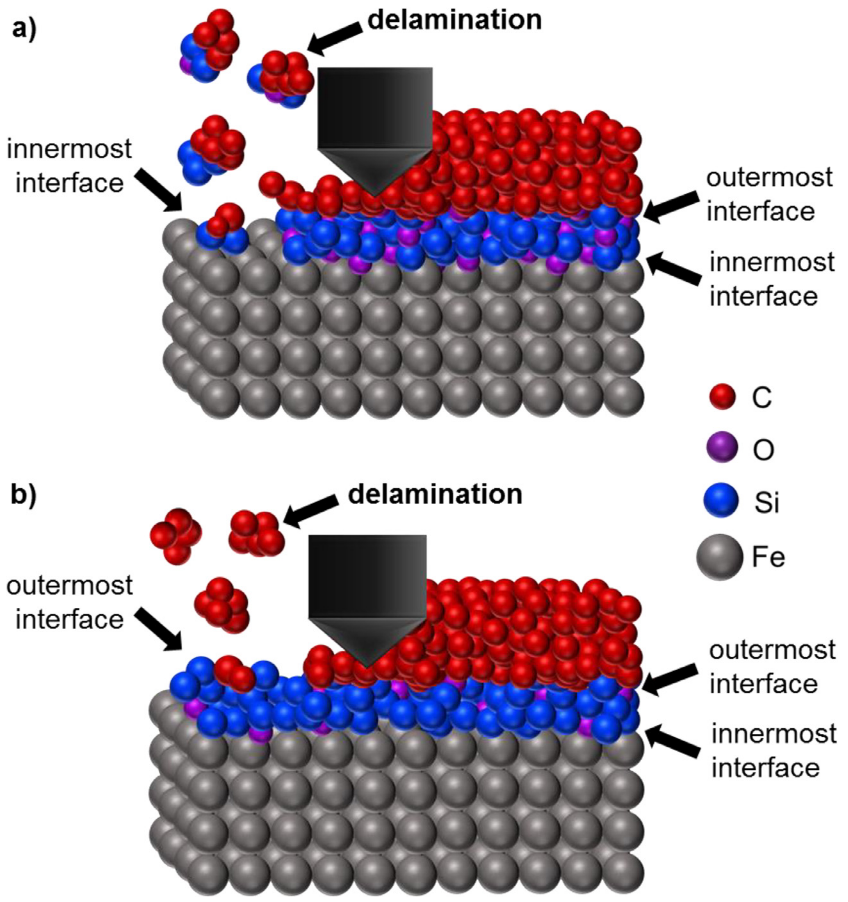

Fig. 4. Delamination mechanism of the sandwich structure of thin film//interlayer//steel occurring during scratching in two different failure modes that depend on a) high (10^{-1} and 10^{-2}) or low b) (10^{-3} and 10^{-4}) deposition base pressure where the innermost or outermost interface is broken, respectively.

composition of interlayers and interfaces controls the tribological behaviour as a whole, in particular the presence of oxygen [31,44]. Oxygen atoms are detrimental due to the interruption of chemical bonding at both interfaces that impairs good adhesion of thin films. For the innermost interface (silicon interlayer / steel), Si-Fe bonds are substituted by terminal Si=O and Fe=O bonds [31,44]. For the outermost interface (carbon thin film / silicon interlayer), C-Si bonds are substituted by terminal C = O and Si=O [31,44]. For high base pressure prior to deposition, the higher initial oxygen concentration is able to form more Si=O and Fe=O chemical bonds at the innermost interface than C = O and Si=O chemical bonds at the outermost interface owing to most of oxygen was used in the formation of the first interface (innermost). Such a mechanism allows explaining the premature adhesion failure at the innermost interface in higher base pressures. On the contrary, for low base pressure prior to deposition, the lower initial oxygen concentration forms less Si=O and Fe=O chemical bonds at the innermost interface than for high base pressure. The innermost interface is preserved and the outermost interface fails in lower base pressures. We suggest that the outermost interface may fail in all deposition conditions, however, the premature delamination at the innermost interface in higher base pressures is hiding this behaviour. Although such practical finding is known in the vacuum coaters' community, we have proved the influence of the deposition base pressure on the adhesion behaviour of carbon thin films in a systematic way.

4. Conclusions

A systematic study of the influence of base pressure prior to deposition on the adhesion behaviour of carbon thin film was performed. Different base pressures prior to deposition modify significantly the critical load for delamination of the carbon films in the mentioned system where better adhesion was achieved at lower deposition base pressures following an exponential behaviour. Also, two different failure mechanisms were detected: at higher deposition base pressures, the delamination takes place at the innermost interface (silicon interlayer // steel) and at lower deposition base pressures, the delamination takes place at the outermost interface (carbon thin film // silicon interlayer). These results might be related to the oxygen presence at the interfaces during the deposition process. This finding might be used to adjust the more adequate base pressure prior to deposition in order to enhance the adhesion of carbon thin films on steels in plasma processing.

Declaration of Competing Interest

The authors declare that they have no known competing financial interests or personal relationships that could have appeared to influence the work reported in this paper.

Acknowledgement

The authors are grateful to UCS, INCT-INES (# 554336/2014-0), CAPES to PROSUC (#88887.153304/2017-00) and PDSE (#88881.362240/2019-01) for financial support to C.D.B., CNPq (#422372/2016-1), FAPERGS (# 17/2551- 0001052-3) and Plasmar Tecnologia Ltda. (# 1408-25.51/14-6) for financial support. C.D.B., L.M.L, C.A.F and A.F.M. are CNPq or CAPES fellows. The authors would also like to thank funding from CEMMPRE UIDB/00285/2020 [co-financed via FEDER and FCT (COMPETE)] and the Epipolé Research Group for their willingness to help with this research.

References

[1] X. Li, X. Deng, H. Kousaka, N. Umehara, Comparative study on effects of load and sliding distance on amorphous hydrogenated carbon (a-C:H) coating and tetrahedral amorphous carbon (ta-C) coating under base-oil lubrication condition, Wear 392–393 (2017) 84–92, doi:10.1016/j.wear.2017.09.009.

[2] R. Zahid, M.B.H. Hassan, M. Varman, R.A. Mufti, M.A. Kalam, N.W.B.M. Zulkifli, M. Gulzar, A review on effects of lubricant formulations on tribological performance and boundary lubrication mechanisms of non-doped DLC/DLC contacts, Crit. Rev. Solid State Mater. Sci. 42 (2017) 267–294, doi:10.1080/10408436.2016.1186599.

[3] W. Tillmann, N.F. Lopes Dias, D. Stangier, W. Maus-Friedrichs, R. Gustus, C.A. Thomann, H. Moldenhauer, J. Debus, Improved adhesion of a-C and a-C:H films with a CrC interlayer on 16MnCr5 by HiPIMS-pretreatment, Surf. Coat. Technol. 375 (2019) 877–887, doi:10.1016/j.surfcoat.2019.07.076.

[4] J.F. Braza, T.S. Sudarshan, Tribological behaviour of diamond and diamondlike carbon films: status and prospects, Mater. Sci. Technol. U.K. 8 (1992) 574–581, doi:10.1179/mst.1992.8.7.574.

[5] J. Laumer, S.K. O'Leary, An adhesion analysis of thin carbon films deposited onto curved and flat Ti6Al4V substrates using rf magnetron sputtering and plasma enhanced chemical vapor deposition techniques, J. Mater. Sci. Mater. Electron. 30 (2019) 5185–5193, doi:10.1007/s10854-019-00817-z.

[6] M. Huang, X. Zhang, P. Ke, A. Wang, Graphite-like carbon films by high power impulse magnetron sputtering, Appl. Surf. Sci. 283 (2013) 321–326, doi:10.1016/j.apsusc.2013.06.109.

[7] P. Kumar, M. Gupta, U.P. Deshpande, D.M. Phase, V. Ganesan, J. Stahn, Density and microstructure of a-C thin films, Diam. Relat. Mater. 84 (2018) 71–76, doi:10.1016/j.diamond.2018.03.008.

[8] K. Sarakinos, A. Braun, C. Zilkens, S. Mráz, J.M. Schneider, H. Zoubos, P. Patsalas, Exploring the potential of high power impulse magnetron sputtering for growth of diamond-like carbon films, Surf. Coat. Technol. 206 (2012) 2706–2710, doi:10.1016/j.surfcoat.2011.11.032.

[9] J. Lin, W.D. Sproul, R. Wei, R. Chistyakov, Diamond like carbon films deposited by HiPIMS using oscillatory voltage pulses, Surf. Coat. Technol. 258 (2014) 1212–1222, doi:10.1016/j.surfcoat.2014.06.061.

[10] S. Nakao, K. Yukimura, S. Nakano, H. Ogiso, DLC coating by HiPIMS: the influence of substrate bias voltage, IEEE Trans. Plasma Sci. 41 (2013) 1819–1829, doi:10.1109/TPS.2013.2256800.

[11] M. Lattemann, B. Abendroth, A. Moafi, D.G. McCulloch, D.R. McKenzie, Controlled glow to arc transition in sputtering for high rate deposition of carbon films, Diam. Relat. Mater. 20 (2011) 68–74, doi:10.1016/j.diamond.2010.11.007.

[12] C.D. Boeira, L.M. Leidens, Â.E. Crespi, M.E.H. Maia da Costa, C.A. Figueroa, A.F. Michels, Adhesion of hydrogenated amorphous carbon films on ferrous alloy by intermediate nitrogen plasma treatment in silicon-containing interlayers, Vacuum 167 (2019) 21–27, doi:10.1016/j.vacuum.2019.05.019.

[13] M.D. Bentzon, K. Mogensen, J.B. Hansen, C. Barholm-Hansen, C. Træholt, P. Holiday, S.S. Eskildsen, Metallic interlayers between steel and diamond-like carbon, Surf. Coat. Technol. 68–69 (1994) 651–655, doi:10.1016/0257-8972(94)90232-1.

[14] T.W.S.S.V Prasad, Solid lubricants : a review, J. Mater. Sci. (2013) 511–531, doi:10.1007/s10853-012-7038-2.

[15] Y. Shibata, T. Kimura, S. Nakao, K. Azuma, Preparation of silicon-doped diamond-like carbon films with electrical conductivity by reactive high-power impulse magnetron sputtering combined with a plasma-based ion implantation system, Diam. Relat. Mater. 101 (2020) 107635, doi:10.1016/j.diamond.2019.107635.

[16] S. Zhang, B. Wang, J.Y. Tang, Processing and characterisation of diamondlike carbon films, Surf. Eng. 13 (1997) 303–309, doi:10.1179/sur.1997.13.4.303.

[17] C.L. Chang, D.Y. Wang, Microstructure and adhesion characteristics of diamond-like carbon films deposited on steel substrates, Diam. Relat. Mater. 10 (2001) 1528–1534, doi:10.1016/S0925-9635(01)00382-X.

[18] B.H. Lung, M.J. Chiang, M.H. Hon, Effect of gradient a-SiCx interlayer on adhesion of DLC films, Mater. Chem. Phys. 72 (2001) 163–166, doi:10.1016/S0254-0584(01)00428-X.

[19] L.F. Bonetti, G. Capote, L.V. Santos, E.J. Corat, V.J. Trava-Airoldi, Adhesion studies of diamond-like carbon films deposited on Ti6Al4V substrate with a silicon interlayer, Thin Solid Films 515 (2006) 375–379, doi:10.1016/J.TSF.2005.12.154.

[20] A. Tyagi, R.S. Walia, Q. Murtaza, S.M. Pandey, P.K. Tyagi, B. Bajaj, A critical review of diamond like carbon coating for wear resistance applications, Int. J. Refract. Met. Hard Mater. 78 (2019) 107–122, doi:10.1016/j.ijrmhm.2018.09.006.

[21] A. Grill, B. Meyerson, V. Patel, Interface modifications for improving the adhesion of a-C : H films to metals, J. Mater. Res. 3 (1988) 214–217, doi:10.1557/JMR.1988.0214.

[22] Q. Chen, C. Zeng, M. Xu, H. Yuan, H. Lv, Z. Wang, X. Wang, Effect of SiN x interlayer thickness on adhesion and friction properties of diamond-like carbon films, Diam. Relat. Mater. 94 (2019) 186–193, doi:10.1016/j.diamond.2019.01.024.

[23] L. Marcinauskas, V. Dovydaitis, A. Iljinas, M. Andrulevičius, Structural and optical properties of doped amorphous carbon films deposited by magnetron sputtering, Thin Solid Films 681 (2019) 15–22, doi:10.1016/j.tsf.2019.04.055.

[24] F. Zhao, H.X. Li, L. Ji, Y.F. Mo, W.L. Quan, H.D. Zhou, J.M. Chen, Structural, mechanical and tribological characterizations of a-C : HH : SSi films prepared by a hybrid PECVD and sputtering technique, J. Phys. D Appl. Phys. (2009) 42, doi:10.1088/0022-3727/42/16/165407.

[25] S. Song, H. Sun, S.C. Chen, M. Dai, K. Wang, X. Zheng, Y. Lu, T. Yang, Z.M. Yue, The adhesion strength and mechanical properties of SiC films deposited on SiAlON buffer layer by magnetron sputtering, Surf. Coat. Technol. 360 (2019) 116–120, doi:10.1016/j.surfcoat.2018.12.115.

[26] M. Evaristo, R. Azevedo, C. Palacio, A. Cavaleiro, Influence of the silicon and oxygen content on the properties of non-hydrogenated amorphous carbon coatings, Diam. Relat. Mater. 70 (2016) 201–210, doi:10.1016/j.diamond.2016.10.024.

[27] S. Nagashima, T. Hasebe, A. Kamijo, Y. Yoshimoto, A. Hotta, H. Morita, H. Terada, M. Tanaka, K. Takahashi, T. Suzuki, Effect of oxygen plasma treatment on non-thrombogenicity of diamond-like carbon films, Diam. Relat. Mater. 19 (2010) 861–865, doi:10.1016/j.diamond.2010.02.003.

[28] D. Feldiorean, D. Cristea, M. Tierean, C. Croitoru, C. Gabor, L. Jakab-Farkas, L. Cunha, N.P. Barradas, E. Alves, V. Craciun, A. Marin, C. Moura, J. Leme, M. Socol, D. Craciun, M. Cosnita, D. Munteanu, Deposition temperature influence on the wear behaviour of carbon-based coatings deposited on hardened steel, Appl. Surf. Sci. 475 (2019) 762–773, doi:10.1016/j.apsusc.2019.01.028.

[29] S. Delfani-Abbariki, A. Abdollah-zadeh, S.M.M. Hadavi, M. Abedi, S.M.R. Derakhshandeh, Enhancing the adhesion of diamond-like carbon films to steel substrates using silicon-containing interlayers, Surf. Coat. Technol. 350 (2018) 74–83.

[30] E.R. Petry, C.D. Boeira, F. Cemin, L.M. Leidens, L.T. Bim, D.G. Larrude, M.E.H. Maia da Costa, C.A. Figueroa, Physicochemical structure of SiCx:H to improve DLC adhesion on steel, Surf. Eng. 32 (2016) 779–785, doi:10.1080/02670844.2016.1159277.

[31] F. Cemin, L.T. Bim, L.M. Leidens, M. Morales, I.J.R. Baumvol, F. Alvarez, C.A. Figueroa, Identification of the chemical bonding prompting adhesion of aC: H thin films on ferrous alloy Intermediated by a SiC x: H buffer layer, ACS Appl. Mater. Interfaces 7 (2015) 15909–15917.

[32] C.D. Boeira, L.M. Leidens, F. Cemin, E.R. Petry, M.E.H. Maia, S.S.C. Jr, A comprehensive study on different silicon-containing interlayers for a-C : H adhesion on ferrous alloys, Thin Solid Films 645 (2018) 351–357, doi:10.1016/j.tsf.2017.10.043.

[33] L.M. Leidens, Â.E. Crespi, C.D. Boeira, F.G. Echeverrigaray, C.A. Figueroa, Hydrogen plasma etching mechanism at the a-C:H/a-SiC x :H interface: a key factor for a-C:H adhesion, Appl. Surf. Sci. (2018), doi:10.1016/j.apsusc.2018.05.203.

[34] F. Ferreira, A. Aijaz, T. Kubart, A. Cavaleiro, J. Oliveira, Surface & Coatings Technology Hard and dense diamond like carbon coatings deposited by deep oscillations magnetron sputtering, Surf. Coat. Technol. 336 (2018) 92–98, doi:10.1016/j.surfcoat.2017.10.055.

[35] A. Escudeiro, T. Polcar, A. Cavaleiro, Tribological behaviour a-C and a-C : H films doped with Ti in biological solutions, Vaccum 85 (2011) 1144–1148, doi:10.1016/j.vacuum.2011.03.011.

[36] V. D. I. Normen, VDI 3198 VDI-Verlag, Dusseldorf, (1991).

[37] S.V. Hainsworth, N.J. Uhure, Diamond like carbon coatings for tribology: production techniques, characterisation methods and applications, Int. Mater. Rev. 52 (2007) 153–174, doi:10.1179/174328007X160272.

[38] European standard UNI EN 1071-3, Advanced technical ceramics methods of test for ceramic coatings part 3: determination of adhesion and other mechanical failure modes by a scratch TestTitle, (2005).

[39] N. Vidakis, A. Antoniadis, N. Bilalis, The VDI 3198 indentation test evaluation of a reliable qualitative control for layered compounds, J. Mater. Process. Technol. 143–144 (2003) 481–485, doi:10.1016/S0924-0136(03)00300-5.

[40] E. Broitman, L. Hultman, Adhesion improvement of carbon-based coatings through a high ionization deposition technique, J. Phys. Conf. Ser. (2012) 370, doi:10.1088/1742-6596/370/1/012009.

[41] J.I. Goldstein, D.E. Newbury, J.R. Michael, N.W.M. Ritchie, J.H.J. Scott, D.C. Joy, Scanning Electron Microscopy and X-Ray Microanalysis, Springer, 2017.

[42] N. Yoshimura, Water vapor permeation through Viton O ring seals, J. Vac. Sci. Technol. A Vac. Surf. Films 7 (1989) 110–112, doi:10.1116/1.575756.

[43] F. Cemin, C.D. Boeira, C.A. Figueroa, On the understanding of the silicon-containing adhesion interlayer in DLC deposited on steel, Tribol. Int. 94 (2016) 464–469, doi:10.1016/J.TRIBOINT.2015.09.044.

[44] A.E. Crespi, L.M. Leidens, V. Antunes, B.L. Perotti, A.F. Michels, F. Alvarez, C.A. Figueroa, Substrate bias voltage tailoring the interfacial chemistry of a-SiCx:H: a surprising improvement in adhesion of a-C:H thin films deposited on ferrous alloys controlled by oxygen, ACS Appl. Mater. Interfaces 11 (2019) 18024–18033, doi:10.1021/acsami.9b03597.